Zeitschrift: Schweizerische mineralogische und petrographische Mitteilungen = Bulletin suisse de minéralogie et pétrographie

Band: 69 (1989)

Heft: 3

Artikel: Pre-Hercynian magmatism in the Eastern Alps : the origin of metabasites from the Austroalpine basement

Autor: Poli, Stefano

DOI: https://doi.org/10.5169/seals-52803

SCHWEIZ. MINERAL. PETROGR. MITT. 69,407–421, 1989

Pre-Hercynian magmatism in the Eastern Alps: the origin of metabasites from the Austroalpine basement

by *Stefano Poli*[1]

Abstract

The paper concerns with the nature of metabasites from the Austroalpine crystalline basement. The metabasites furnish fundamental information on the pre-Variscan history of the Austroalpine terrain as they were metamorphosed in the amphibolite facies by the Hercynian orogenesis.

Major and trace element analyses (including REE, Ta, Nb, Zr, Y) were carried out on 60 selected metabasites from the Southern Oetztal and Languard-Campo units of the Central Austroalpine crystalline basement. The alkaline and alkaline-earth element mobility and, when necessary, the sedimentary contamination were qualitatively assessed by interpreting the petrographic data (e.g. carbonates) and the self-consistency of mantle normalized patterns.

At least three magmatic series were recognized :

– NNW metabasalts (Roja, Melag, Central Venosta and Passiria valleys) have high TiO_2 (1.8%–2.7%), high Ta/La and Zr/Y ratios. These data demonstrate their affinity to the Within Plate Basalts. This conclusion is strengthened by a 15%–20% equilibrium partial melting model of a garnet-bearing mantle source.

– Mt. Vertana metabasalts have low TiO_2 (1%–1.3%) and relatively high Al_2O_3 (16%–17%). Their calcalkaline affinity is substantiated by Ta, Nb, P negative anomalies. These same features are apparently shared by the least fractionated (Cr=440 ppm) samples of Pennes gabbro body.

– Very low TiO_2 value (0.4%-1%), distinct Ta, Nb, P and Hf negative anomalies, LREE enrichment coupled to HREE depletion lead to the conclusion that the Fleres meta-andesites were directly related to destructive plate margins.

The coexistence of anorogenic and orogenic magmatism in the Oetztal-Campo basement can be alternatively referred either to the tectonic evolution from a distensive to a compressive plate margin or to the coeval emission in a marginal or back-arc basin. The apparent lack of Ocean Floor Basalts, the affinity of NNW metabasites to Within Plate Basalts and the very limited volume occupied by the metabasites within the metapelitic Austroalpine basement suggest that there was no development of a large ocean basin prior to the Hercynian orogenesis. On the basis of existing data, the Fleres andesites may represent either a pre- or a sin-Hercynian magmatic event.

Keywords: Amphibolites, bulk rock chemistry, trace elements, geodynamics, pre-Hercynian, Austroalpine.

Introduction

Hercynian metamorphism and, locally, Alpine overprint have greatly complicated the reconstruction of the pre-Variscan history of Austroalpine crystalline basement (GREGNANIN and PICCIRILLO 1972, 1974; GREGNANIN 1980; FRANK et al. 1987a).

Investigation of the igneous rocks within the basement has improved the knowledge of the (pre-)Palaeozoic geodynamics in the Austroalpine domain. Early Palaeozoic («Caledonian») acid magmatism in the Eastern Alps is recorded by Upper Ordovician granitoids, dated ≈450-440 m.y. (SASSI et al., 1985), and by rhyolitic «porphyrites» (BELLIENI and SASSI, 1981). Apart from the MOGESSIE et al.'s (1985) investigation of some basic intercalations in the metamorphic basement of Oetztal-Stubai complex, very few chemical data are available for mafic rocks,

[1] Dipartimento Scienze della Terra, Via Botticelli 23, I-20133 Milano, Italy.

especially on the Southern Oetztal and Languard-Campo units of the Austroalpine domain.

In this study, basic rocks, mainly metamorphosed in the Hercynian amphibolite facies, are considered. Field study, petrography and major and trace element (including REE, Ta, Nb, Zr and Y) analyses allowed us to select some igneous bodies and to make some inferences about their genesis.

Geological framework

The area investigated (Fig. 1) is a part of the Oetztal-Campo crystalline basement of the Upper Austroalpine unit (DAL PIAZ, 1936). The pre-Permian metasedimentary Oetztal-Campo basement, between the Tonale-Giudicarie line and the northern Italian frontier, is divided, according to GREGNANIN and PICCIRILLO (1972, 1974), into two main complexes. The deepest ter-

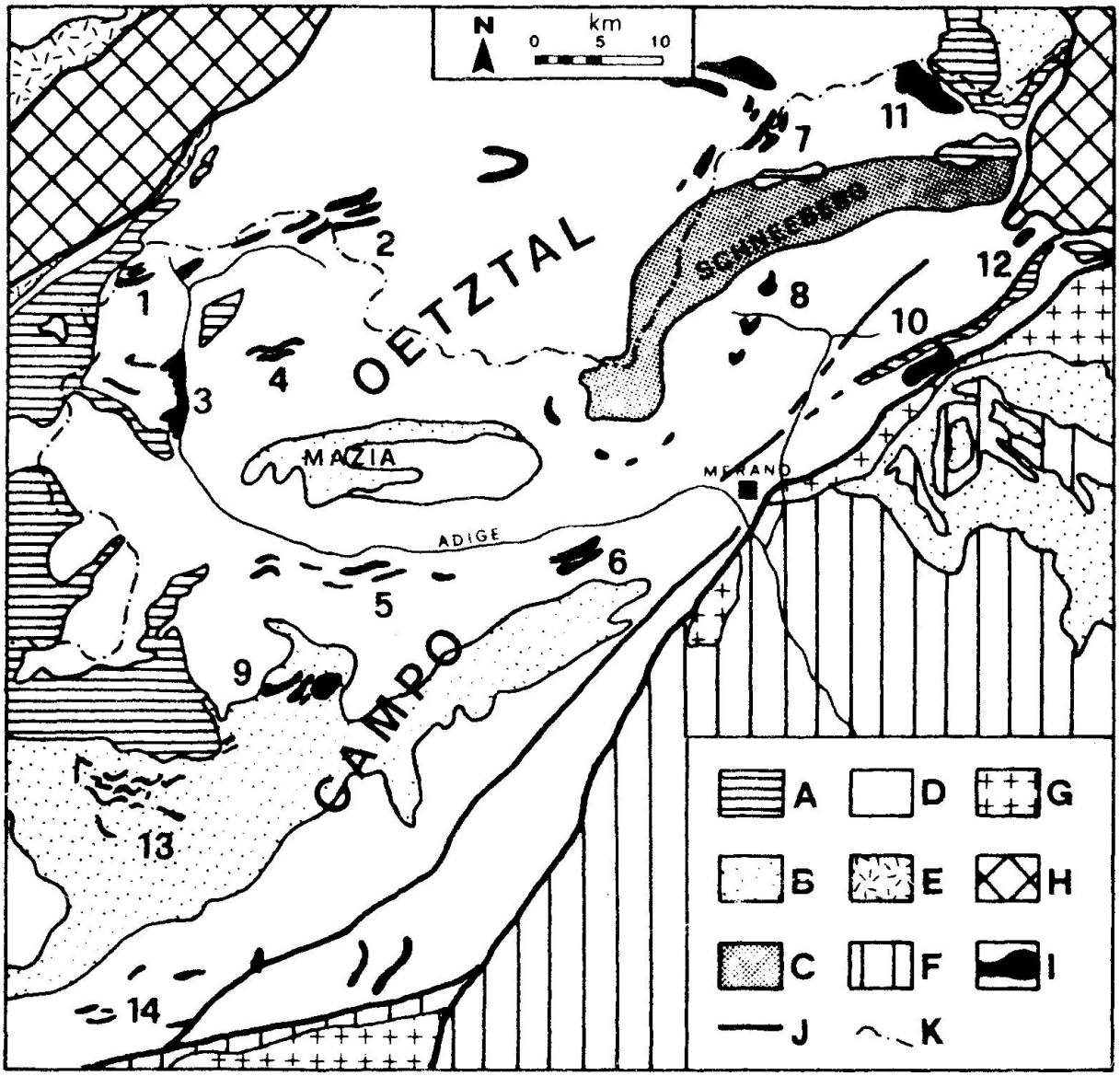

Fig. 1 Geological sketch map of the Austroalpine domain studied (after GREGNANIN, 1980). A = sedimentary Austroalpine cover; B = pre-Permian phyllites; C = Schneeberg crystalline; D = Oetztal-Campo-Tonale complex; E = Lower Austroalpine crystalline; F = Southalpine domain; G = periadriatic intrusions; H = Pennine domain; I = amphibolitic bodies; J = tectonic lines; K = italian boundary line. Numbers represent sample locations. Labels in parentheses in the following list refer to sample labels in Tables. 1 - Roja valley (ROJ); 2 - Melag valleys (MEL); 3 - Burgusio (BUR and CLU); 4 - Mt. Zerzerkopfl (ZE); 5 - Central Venosta valley (LASA and COV); 6 - Laces (LAC); 7 - Timmel valley (TUM); 8 - Moso, Passiria valley (MOS); 9 - Mt. Vertana (VERT and VMAR); 10 - Pennes valley (COBI); 11 - Fleres valley (FLE); 12 - Elzenbaum (ELZ); 13 - Zebrù valley (VZ); 14 - Camonica and Sole valleys (VMS, MAS and 78T).

rain is represented by the "banded paragneisses" (BAGGIO et al., 1971) which are the result of the metamorphism of a flysch-type series, with intercalations of basic rocks, granitoids and pegmatites. The upper complex, the "phyllites s.l.", is mainly pelitic with minor amounts of basic rocks and granitoids. The boundary between these two formations is transitional (the "silver micaschists") and it is characterized by the presence of marbles, often associated with amphibolites and quarzites.

According to GREGNANIN (1980), both the banded paragneisses and the phyllites have the same metamorphic history. FRANK et al. (1987b) report whole-rock ages on orthogneisses of 450-420 m.y. (Caledonian magmatism) and Rb/Sr mica ages ranging from 350 to 10 m.y. (Hercynian and Alpine orogeneses). The upper thermal limits reached in the Hercynian are recorded by the Winnebach migmatite in the northern Oetztal complex (HOINKES et al., 1972) and by the sillimanite + muscovite + plagioclase assemblage in the Campo complex (GREGNANIN and PICCIRILLO, 1972). The Alpine event was marked by a widespread retrogression of staurolite to chloritoid and, locally (in the Texelgruppe, FRANK et al., 1987a), by a second generation of staurolite.

The overprinting of two (GREGNANIN and PICCIRILLO, 1974) or three (FRANK et al., 1987a) pre-Alpine (probably Hercynian) phases of deformation caused the kilometre-scale folds, which have steep fold-axes, known as the «Schlingentektonik» or «Vortex tectonic» (SANDER, 1912). The Alpine metamorphic event is associated with a subordinated deformation phase.

The metabasites under consideration are conformably inter-bedded with banded paragneisses, silver mica-schists and phyllites. Since all of these rocks were metamorphosed by the Hercynian event, the metabasic layers have been emplaced in pre-Hercynian times.

Mineral assemblages are usually rather uniform and comprise amphibole (hornblende and/or actinolite) + plagioclase + epidote + quartz ± chlorite ± garnet ± biotite (COMMON assemblage, LAIRD and ALBEE, 1981). Metamorphic diopside (unpublished electron microprobe data) was found in amphibolites of the Tonale series and in Mt. Vertana metabasites. Relic eclogite assemblage (garnet 20% pyrope, clinopyroxene 25% jadeite, clinozoisite, barroisite) is recorded in the amphibolites at Moso in Passiria valley. Within the Oetztal-Campo crystalline basement, the Pennes gabbro (Fig. 2) provide the only good example of preserved magmatic textures. Sample locations are given in Fig. 1.

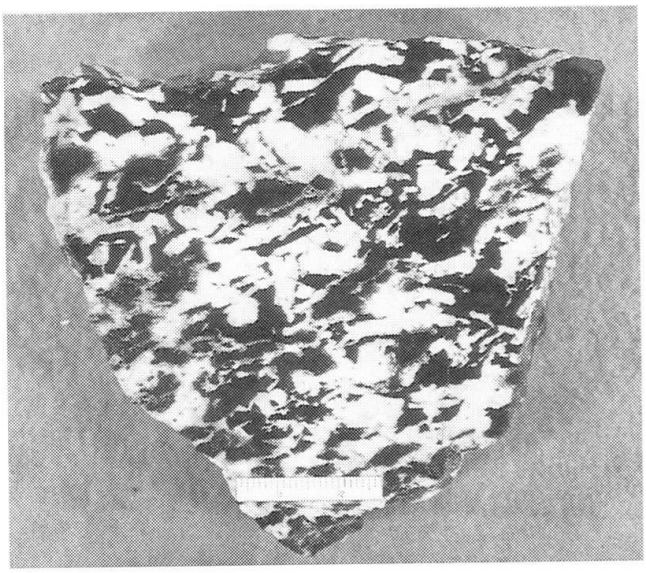

Fig. 2 A rare example of relic magmatic textures in pre-Hercynian metabasites from the Austroalpine terrain: a slightly deformed plagioclase orthocumulate from Pennes gabbro.

Analytical techniques

The samples were ground in an agate mortar. Na_2O, K_2O, MgO and MnO were determined by Atomic Absorption Spectrometry (AAS), while SiO_2, Al_2O_3, Fe_2O_3, CaO, TiO_2 and P_2O_5 were determined by X-Ray Fluorescence (XRF). FeO was obtained by titration with $KMnO_4$.

Trace elements were measured using the following methods:

a) XRF for V, Cr, Rb, Sr, Y, Zr, Nb on glasses using $LiBO_2$ as a flux. Twenty certified international standards plus synthetic standards were used in order to calculate the corrections for matrix effects. The analytical errors are estimated at 10%.

b) Instrumental Neutron Activation Analysis (INAA) for Sc, Cr, Co, Cs, Ba, La, Ce, Nd, Sm, Eu, Tb, Yb, Lu, Hf, Ta, Th, U at the Centre des Faibles Radioactivités (Gif sur Yvette, France). Samples were held in ultrapure silica capsules and were irradiated with a flux of 2×10^{14} n cm $^{-2}$ s^{-1} for 25 min, at the Osiris reactor (Centre Etudes Nucléaires, Saclay, France), using GSN and BEN standards. The uncertainties are : Sc, Co, Cs, La, Ce, Sm, Eu, Tb, Yb, Hf, Ta and Th 10%; Cr, Ba, Nd and Lu 15%; U 20%.

The results of 46 selected determinations of major and trace elements by XRF and AAS are reported in Tab. 1; trace elements by INAA on 15 selected samples are listed in Tab. 2.

Tab. 1 Major and XRF trace element composition of metabasites from the Austroalpine domain. Keys refer to location of samples in Fig. 1 (see caption):
a) NNW amphibolites - Δ in figures.

Sample	ROJ 2	ROJ 3	MEL 1	MEL 4	MEL 5	MEL 6	BUR 3	BUR 5	BUR 7	BUR 8	CLU
Key	1	1	2	2	2	2	3	3	3	3	3
SiO_2	48.90	47.00	48.00	48.45	46.10	47.70	43.80	49.00	45.85	47.00	47.80
TiO_2	2.53	2.37	1.75	2.07	1.85	1.52	1.97	2.55	2.03	1.94	2.10
Al_2O_3	14.10	18.30	15.00	15.00	19.10	18.80	14.20	13.90	14.80	15.70	16.90
Fe_2O_3	3.04	4.83	0.75	0.00	4.01	1.43	2.53	3.57	2.30	2.12	2.78
FeO	8.74	3.39	10.01	10.30	5.93	7.35	7.71	8.57	8.28	8.17	8.44
MnO	0.23	0.16	0.20	0.23	0.17	0.12	0.24	0.21	0.18	0.18	0.28
MgO	6.58	2.33	6.79	6.79	6.67	4.50	4.47	6.14	7.52	8.22	4.70
CaO	10.30	10.26	9.47	10.45	8.50	10.08	11.31	8.07	11.06	10.50	8.77
Na_2O	2.35	4.15	2.81	3.41	3.52	3.34	3.66	4.21	2.97	2.90	3.87
K_2O	0.75	1.81	1.22	0.42	0.75	1.53	0.89	0.52	0.59	0.58	0.99
P_2O_5	0.27	0.60	0.19	0.21	0.21	0.14	0.26	0.25	0.25	0.21	0.17
H_2O+	2.32	4.43	2.70	2.21	2.62	3.13	7.07	2.64	3.94	2.22	3.01
Total	100.11	99.63	98.89	99.54	99.43	99.64	98.11	99.63	99.77	99.74	99.81
Mgv	54.0	43.7	54.0	54.0	61.1	50.3	47.7	52.2	59.3	61.9	46.7
Cr	178	140	300	310	129	142	71	61	241	283	301
Rb	25	49	49	10	21	48	18	8	16	16	26
Sr	218	520	219	176	273	356	221	170	206	207	274
Y	38	28	31	28	22	21	20	27	29	32	32
Zr	173	250	133	147	104	112	118	181	149	158	160
Nb	9	55	11	15	18	12	20	18	12	9	10

Sample	ZE 1	ZE 5	LAC1	LAC 2	LAC2B	TUM 1	TUM 2	MOS 1	MOS2	MOS 3	MOS 4
Key	4	4	6	6	6	7	7	8	8	8	8
SiO_2	47.65	46.35	48.10	49.70	47.40	47.10	49.60	48.50	46.40	47.30	49.00
TiO_2	1.74	2.22	2.27	2.33	2.03	2.10	1.59	1.90	1.77	1.11	1.91
Al_2O_3	16.39	14.15	16.04	16.45	16.25	15.75	17.49	15.05	15.58	16.20	15.00
Fe_2O_3	1.50	0.77	6.09	3.33	2.48	2.72	0.66	2.71	1.36	1.73	4.07
FeO	8.53	9.68	6.36	8.70	8.35	7.65	8.62	7.37	8.34	8.08	6.62
MnO	0.18	0.19	0.22	0.22	0.20	0.21	0.11	0.19	0.20	0.15	0.21
MgO	6.60	6.29	4.08	3.90	6.39	4.43	7.76	7.03	4.92	5.25	6.90
CaO	10.58	12.12	9.32	9.06	10.85	11.12	6.80	10.43	12.26	11.45	10.14
Na_2O	3.22	2.72	4.13	4.21	3.10	4.49	3.39	3.51	2.85	3.53	3.73
K_2O	0.75	1.01	0.58	0.57	0.46	0.28	1.33	0.17	0.63	0.91	0.20
P_2O_5	0.27	0.28	0.27	0.22	0.28	0.22	0.16	0.20	0.25	0.10	0.24
H_2O+	2.40	3.66	1.68	1.59	1.77	3.30	2.15	1.32	4.63	3.78	1.72
Total	99.81	99.44	99.14	100.28	99.56	99.37	99.66	98.38	99.19	99.59	99.74
Mgv	56.3	52.9	45.2	40.9	54.9	47.4	60.9	59.7	49.7	51.6	59.8
Cr	278	265	309	345	347	323	177	270	319	274	206
Rb	18	24	14	19	10	3	55	2	16	27	5
Sr	291	350	188	214	281	249	212	207	236	180	239
Y	21	26	27	36	29	28	30	24	28	35	29
Zr	121	161	146	182	158	147	148	127	145	162	158
Nb	24	23	9	12	16	11	6	12	12	13	14

b) Vertana amphibolites - ● in figures.

Sample	VERT2	VERT3	VERT4	VERT5	VERT6	VMAR1	VMAR2	VMAR8	VMAR9	VMA12
Key	9	9	9	9	9	9	9	9	9	9
SiO_2	46.85	46.23	48.70	49.30	48.20	44.80	46.45	49.90	49.40	48.05
TiO_2	1.47	1.08	1.11	1.86	1.14	1.16	1.11	1.04	1.05	1.26
Al_2O_3	16.05	16.20	16.00	14.45	16.70	15.75	15.95	16.50	16.50	16.90
Fe_2O_3	1.63	1.33	0.80	1.73	1.60	1.08	1.52	0.74	0.74	0.61
FeO	8.13	9.13	10.08	8.89	8.37	8.69	8.33	8.65	8.68	10.25
MnO	0.19	0.19	0.20	0.16	0.15	0.18	0.20	0.16	0.17	0.16
MgO	4.72	8.53	7.12	6.45	5.09	7.51	7.09	6.93	7.85	4.92
CaO	12.48	12.22	10.34	11.58	14.23	14.05	13.05	9.66	10.87	12.45
Na_2O	3.53	1.94	3.33	2.95	2.82	2.05	2.30	3.69	2.96	3.00
K_2O	0.49	0.59	0.28	0.42	0.29	0.55	0.22	0.46	0.16	0.51
P_2O_5	0.21	0.07	0.06	0.18	0.11	0.08	0.07	0.08	0.07	0.08
H_2O+	3.93	2.56	1.71	1.89	1.78	3.90	3.35	1.85	1.51	1.40
Total	99.68	100.07	99.73	99.86	100.48	99.80	99.64	99.66	99.96	99.59
Mgv	48.9	61.1	54.9	54.5	50.1	59.4	58.5	58.0	60.9	45.5
Cr	212	322	311	316	238	255	261	275	307	385
Rb	12	33	7	14	5	20	9	16	5	4
Sr	286	163	286	227	294	231	262	212	257	329
Y	21	26	23	24	23	21	22	22	22	24
Zr	124	92	105	133	95	108	90	93	81	116
Nb	14	4	4	14	6	4	4	5	4	7

c) Pennes metagabbro - ✱ in figures.

Sample	COBI1	COBI3	COBI5	COB13A	COB15	COB18	COB19
Key	10	10	10	10	10	10	10
SiO_2	48.75	49.50	50.00	50.40	46.63	50.04	46.62
TiO_2	0.19	0.18	0.68	0.35	1.34	1.01	1.28
Al_2O_3	19.10	17.45	15.65	19.90	14.25	18.53	14.52
Fe_2O_3	0.00	0.42	0.04	5.75	12.13	10.72	11.96
FeO	6.47	6.06	8.34	0.00	0.00	0.00	0.00
MnO	0.11	0.11	0.19	0.10	0.20	0.20	0.19
MgO	9.51	10.00	8.84	7.55	9.20	5.25	8.54
CaO	9.59	10.02	11.25	11.10	13.04	9.32	12.86
Na_2O	3.17	2.41	2.30	2.62	2.08	3.24	2.22
K_2O	0.50	0.62	0.34	1.20	0.07	0.67	0.06
P_2O_5	0.02	0.02	0.02	0.02	0.02	0.17	0.02
H_2O+	2.47	2.76	2.00	1.94	1.18	1.10	1.29
Total	99.88	99.55	99.65	100.93	100.14	100.25	99.56
Mgv	72.4	74.1	65.3	85.2	76.9	68.3	75.9
Cr	220	186	446	376	349	66	317
Rb	21	28	7	61	1	17	1
Sr	281	191	268	285	126	550	143
Y	10	10	12	18	21	21	22
Zr	27	26	36	54	44	112	47
Nb	2	2	2	3	3	6	2

d) Fleres and Elzenbaum meta-andesites - ⊡ and < in figures.

Sample	FLE 1	FLE 4	FLE 5	FLE 7	FLE19	ELZ 1	ELZ 2
Key	11	11	11	11	11	12	12
SiO_2	57.60	57.25	55.75	59.50	56.89	60.70	61.55
TiO_2	0.90	0.46	0.49	0.87	0.98	0.53	0.50
Al_2O_3	16.45	14.50	15.90	16.40	16.84	15.35	15.90
Fe_2O_3	0.48	0.66	0.40	4.81	9.38	0.75	0.76
FeO	7.16	7.11	7.41	3.07	0.00	5.73	5.40
MnO	0.12	0.17	0.12	0.13	0.15	0.13	0.12
MgO	3.55	7.58	6.22	2.90	3.43	3.82	3.25
CaO	7.37	6.52	7.07	5.54	6.60	6.88	6.53
Na_2O	2.40	1.62	1.58	3.29	2.24	3.02	3.30
K_2O	1.40	1.62	1.05	1.61	1.61	0.77	0.92
P_2O_5	0.09	0.05	0.16	0.10	0.16	0.05	0.06
H_2O+	2.31	2.34	3.83	1.50	1.29	1.57	1.41
Total	99.83	99.88	99.98	99.72	99.57	99.30	99.70
Mgv	46.2	64.7	53.4	50.7	61.7	53.0	50.4
Cr	66	381	161	32	33	70	48
Rb	54	58	32	52	55	15	23
Sr	473	137	207	412	217	227	268
Y	20	20	16	23	30	14	17
Zr	91	68	72	115	190	102	116
Nb	7	6	5	8	9	5	4

Results

A major problem in the study of metabasites in a (poly)metamorphic terrain is to distinguish between ortho- and para-amphibolites. Field observation, e.g. of the shape, thickness of the mafic bodies, their homogeneity, the sharpness of the boundaries, banding, relics of magmatic textures are very useful for a preliminary division. Petrographic observation, such as the presence of carbonates, and chemical data can provide important information in refining this subdivision.

Whereas the term ortho-derivative embraces all clearly magmatic rocks, the term para-derivative groups both mixtures of dolomite-limestone-shale (LEAKE, 1964), and volcaniclastic sediments (e.g. tuffs). Since metabasites interlayered with marbles were not considered in this study, the recognized para-amphibolites are probably either (volcaniclastic) litharenites or pyroclastic products interlayered with clastic sediments, such as are now found in the western Mediterranean (PATERNE et al., 1986). In both of these cases, chemical data may be affected by contamination

Tab. 2 Trace element by INAA. Samples and keys as in Fig. 1 and Tab. 1.

Sample	ROJ3	MEL 1	BUR 5	BUR 8	LAC 2	MOS 4	VERT3	VERT6	VMAR8
Key	1	2	3	3	6	8	9	9	9
Sc	22	39	37	33	41	39	33	32	32
Co	34	43	41	42	43	42	53	46	41
Ni	71	53	27	170	96	78	160	135	125
Cs	0.7	0.5	0.2	0.5	2.6	0.2	2.7	1.5	8.8
Ba	510	230	153	70	120	70	130	90	48
La	35.0	11.0	17.0	10.0	11.0	11.0	6.1	5.7	8.7
Ce	80.0	27.0	41.0	24.0	27.0	28.0	15.0	14.0	18.0
Nd	31.0	17.0	25.0	18.0	20.0	20.0	11.0	9.3	12.0
Sm	5.5	4.1	6.1	4.9	5.1	4.8	2.6	2.5	3.0
Eu	2.15	1.50	2.10	1.60	1.90	1.80	1.15	1.02	1.00
Tb	0.86	0.96	1.20	1.00	1.25	1.20	0.58	0.66	0.65
Yb	2.60	3.30	3.00	3.30	4.00	3.70	2.26	2.20	2.30
Lu	0.50	0.48	0.46	0.50	0.62	0.60	0.38	0.35	0.34
Hf	5.60	3.50	4.50	3.60	4.40	4.00	2.00	2.10	2.10
Ta	4.70	0.60	1.30	0.50	0.56	0.80	0.22	0.20	0.30
Th	5.50	1.10	1.60	1.10	0.72	1.10	1.10	0.75	1.80
U	1.5	0.3	0.4	0.2	0.2	0.3	0.4	0.1	0.6

Sample	COBI1	COBI3	COBI5	FLE 1	FLE 4	FLE 5	FLE 7	ELZ 2
Key	10	10	10	11	11	11	11	12
Sc	16	180	40	28	30	30	25	21
Co	42	47	40	17	32	27	18	19
Ni	50	100	23	13	80	42	15	30
Cs	1.2	1.3	0.3	1.6	2.3	2.6	3.4	0.9
Ba	100	146	100	480	340	220	420	440
La	0.9	0.7	6.2	18.0	14.0	14.0	22.0	15.0
Ce	1.8	1.5	13.0	33.0	28.0	27.0	43.0	28.0
Nd	1.1	1.0	5.4	15.0	12.0	12.0	21.0	13.0
Sm	0.4	0.4	1.3	2.9	2.7	2.4	4.0	2.5
Eu	0.50	0.60	0.80	1.00	0.70	0.80	1.00	0.80
Tb	0.10	0.15	0.25	0.52	0.40	0.43	0.70	0.40
Yb	0.39	0.49	1.00	1.60	1.50	1.30	2.20	1.60
Lu	0.06	0.09	0.15	0.28	0.23	0.20	0.34	0.27
Hf	0.14	0.20	0.70	2.10	1.50	1.90	2.80	2.70
Ta	0.05	0.00	0.10	0.37	0.40	0.30	0.52	0.20
Th	0.10	0.00	1.30	3.60	5.10	4.60	6.90	4.00
U	0.2	0.0	0.6	1.3	1.4	0.9	1.5	1.3

from sediments. Nevertheless, consideration of differentiation trends for both major and trace elements can help verify the internal consistency of the data and to establish whether these trends preserve a magmatic origin. However, we would stress the importance of field observations, being carried out prior to refining the division on the basis of chemical parameters.

SEDIMENTARY CONTAMINATION

In the Zebrù valley (Site 13 on Fig. 1) gradual and repeated transitions between phyllites, chloritic schists and prasinites (chlorite + albite + actinolite + epidote + quartz + carbonates) were displayed in the series. Interlayered carbonates and tourmaline porphyroclasts in prasinites suggest contamination by detrital sediments. It is worth noting that the composition of the prasinites is not abnormal. The Zebrù prasinites are low-Ti tholeiites (Tab. 1). Cr contents ('300 ppm, Tab. 1) were also normal for a slightly differentiated basalt. Some amphibolites from the Venosta valley (e.g. from Covelano, Site 5 on Fig. 1) are characterized by very transitional boundaries and they are usually very thin (from decimetre to metre). Interlayering of leucocratic (plagioclase rich) amphibolites, melanocratic (amphibole rich) amphibolites and amphibolitic paragneisses on a decimetre-scale characterized these metabasites and also those from the Camonica valley. By means of mg*100/c/al-alk plot proposed by LEAKE (1964) (not shown) all of these rocks define a magmatic trend. Nevertheless, the differentiation trend largely crossing

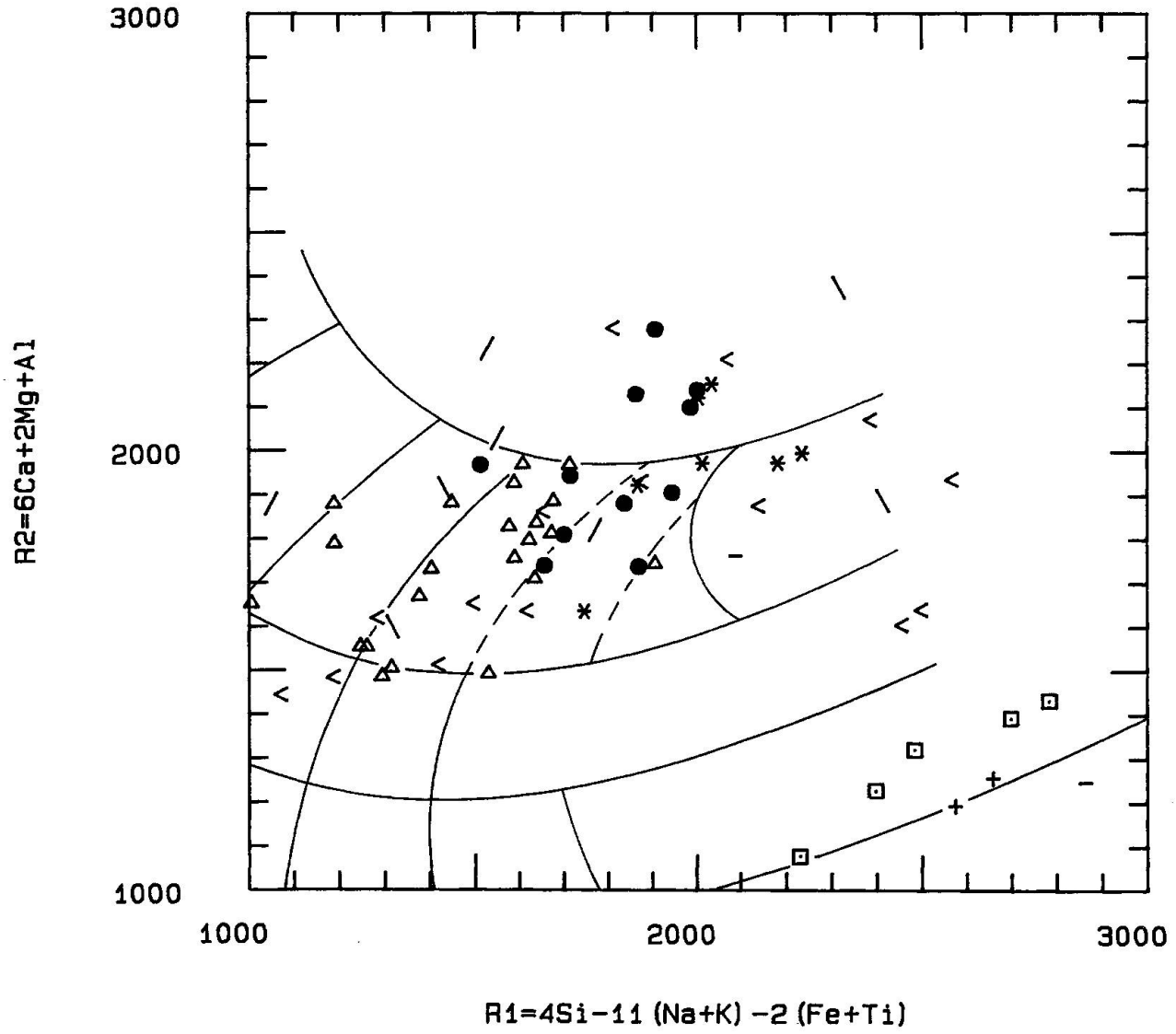

Fig. 3 R1-R2 classification (De La Roche et al., 1980). Symbols: Δ =NNW-amphibolites; ●=Mt. Vertana amphibolites; ✳=Pennes metagabbro; ⊡=Fleres meta-andesites; +=Elzenbaum meta-andesites; /=Valtellina prasinites; \= Camonica valley amphibolites; < = Val di Sole amphibolites.

the silica saturation plane in R1 - R2 diagram (R1=4Si-11(Na+K)-2(Fe+Ti) and R2=Al+2Mg+6Ca; De La Roche et al., 1980), is probably unrelated to a low-pressure differentiation (Fig. 3). Thus, metabasites from the Zebrù, Camonica and Sole valleys and partly those from the Venosta valley (see keys 5, 13, 14 in Tab. 1) were excluded from the discussion due to the probable contamination by sediments.

CHEMICAL MOBILITY

In order to avoid problems due to centimetre scale diffusion and metamorphic differentiation phenomena, 1 to 3 kg samples of rock were crushed and analyzed. Nevertheless, chemical data can be affected by mobilization of large ion element during post-magmatic evolution (Pearce, 1975). A qualitative estimation of the degree to which element migration has occurred may be obtained from the inspection of the Wood's (1979) mantle-normalized diagram (Fig. 4). From Cs to K (Rb), element values are very variable. Cs varies by a factor of 10 whereas K varies by a factor of 3. Trends also frequently cross each other. Thus, these large-ion litophile elements almost certainly were affected by post-magmatic migration. The behaviour of elements with very low bulk solid-liquid partition coefficient (D) may be inferred from that of Th since the Th variation is generally consistent with those of other incompatible immobile elements

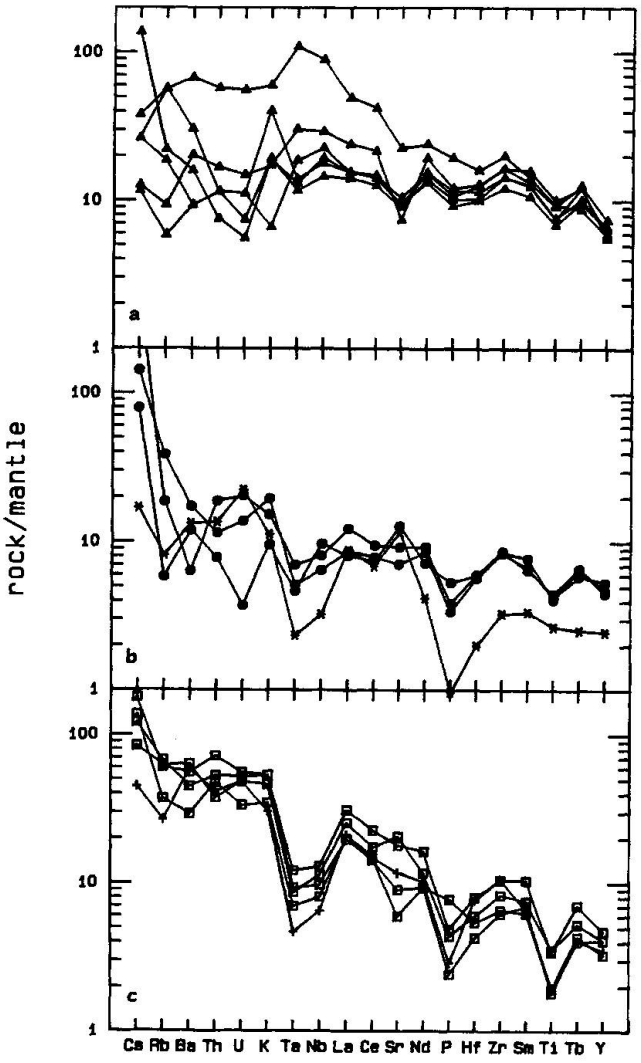

Fig. 4 Mantle normalized diagrams according to WOOD (1979). a) NNW-amphibolites; b) Vertana amphibolites and Pennes gabbro; c) Fleres meta-andesite. Symbols as in Fig. 3.

(e.g. Ta, Hf) during the processes of epidotization and/or carbonization (CONDIE et al., 1977) and spilitization ("coherent mobility" in NYSTROM, 1984). Silica and alkali migration can also be estimated from normative nepheline or hypersthene variations relative to those of an immobile incompatible element such as Zr. No significant positive correlation is observed. Thus, the highest *ne* contents (up to 7%) cannot be related either to low pressure differentiation, or to primary magma features. As a consequence, some of the metabasites from the Oetztal Campo basement are probably displaced slightly towards the alkali-basalt field, in the R1-R2 classificative grid (Fig. 3).

No evidence is found for post-magmatic variation of incompatible elements such as Ta or higher D elements listed in Fig. 4.

The origin of protoliths

The amphibolites selected from the Oetztal-Campo crystalline basement (Key 1 to 12 in Table 1 and 2) have sharp contacts (i.e. centimetre as an order of magnitude) with the metapelitic series; they are generally much thicker (several tens of metres) than those previously described and some resemble slightly flattened intrusive bodies (the Fleres valley body, several hundred metres thick). Carbonates are generally absent. In the Pennes valley gabbro, relic augite and undeformed ophitic textures are visible (Fig. 2).

According to the classificative grid in the R1-R2 diagram (Fig. 3) most samples fall in the basalt field, transitional from sub-alkaline to alkaline. A transitional character was already shown by MOGESSIE et al. (1985) for metabasites from Northern and Central Oetztal. On average, the metabasites from Mt. Vertana are more basic than those from the Venosta and Passiria valleys (Sites 1 to 8 on Fig. 1). A group of samples from the eastern sector of the studied area (the Fleres valley and Elzenbaum) is clearly located in the andesite field. TiO_2 vs Mg-value (calculated according to the «m-value» of HUGHES and HUSSEY, 1976) (Fig. 5) and TiO_2 vs Zr (Fig. 6) plots show a marked subdivision between three groups: a) amphibolites from the northern and northwestern sector (Sites 1 to 8 on Fig. 1) have TiO_2 ranging from about 1.8–2% at ≈60 Mgv - ≈100 ppm Zr up to ≈2.5% at ≈40 Mgv - ≈180 ppm Zr; b) metabasites from Mt. Vertana (Site 9) have TiO_2 generally from 1% at 60 Mgv - 80 ppm Zr to ≈1.3% at 45 Mgv - ≈120 ppm Zr; c) amphibolites from the eastern sector (Fleres and Elzenbaum; Sites 11 and 12) have TiO_2 from ≈0.5 to 1% for Mgv ranging from 65 to 45 and

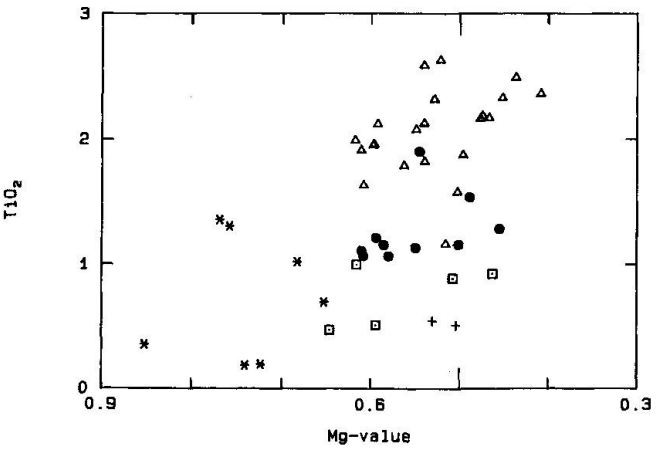

Fig. 5 TiO_2 vs Mg values. Symbols as in Fig. 3.

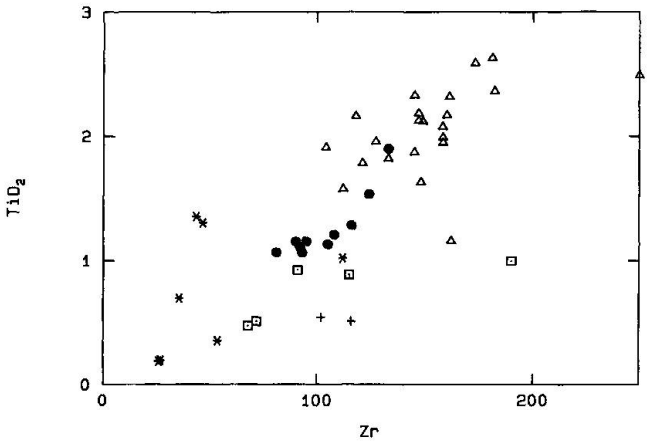

Fig. 6 TiO_2 vs Zr. Symbols as in Fig. 3.

Zr from 70 to 190 ppm; some samples from the Pennes gabbro (Site 10) also have low TiO_2 values and always high Mgv and low Zr abundances (<50 ppm). This subdivision, based on TiO_2 correlates with the grouping based on Ta and Nb anomalies. Therefore, we will discuss separately the group of metabasites from the N-NW sector (the Roja, Melag, central Venosta, Passiria valleys, hereinafter referred to as NNW-amphibolites) which have TiO_2 at ≈2% and the group from Mt. Vertana and the eastern sector (e.g. the Fleres bodies), which has low TiO_2 contents (≤ 1%). As will be discussed below, the former are probably of anorogenic origin and the latter probably genetically related to subduction processes.

THE NNW AMPHIBOLITES: THE ANOROGENIC SERIES

As stated above, NNW amphibolites are transitional basalts on the basis of the R1-R2 grid (Fig. 3). High TiO_2 contents are coupled with variable Al_2O_3. This series displays moderate FeO* enrichment with increasing FeO*/MgO. It is worth noting that the high-Ti Volcanics (HTV) within the Paleozoic sedimentary cover of the Carnian Alps (Sinigoi et al., 1988) are definitely very similar to NNW amphibolites.

The Wood (1979) pattern for most samples is modified slightly by fractional crystallization, because most 3d elements (Fig. 7) of NNW amphibolites lie in the field of least fractionated basalts from the Middle Atlantic Ridge (Langmuir et al., 1977). The slightly low Cr and Ni contents could be related to the small amounts of olivine and clinopyroxene fractionated. Substantial fractional crystallization of plagioclase probably did not occur because there is neither Eu negative anomaly in the chondrite normalized REE plot (Fig. 8a) nor Sr negative anomaly in Wood's pattern (Fig. 4a).

The mantle-normalized pattern (Fig. 4a) is characterized by slight positive anomalies in Ta and Nb, and by a probable absence of low D element enrichment or depletion (see Th values). This pattern, both in absolute value and in trend, confirms a character of the series transitional to alkali-basalts and suggests affinity to E-MORB or to Within Plate Basalt (WPB) type. Differentiation causes enrichment in incompatible elements and Wood's pattern (ROJ3, Mg value=43) strongly resembles an alkali basalt pattern owing to marked Ta and Nb positive anomalies.

Th-Hf/3-Ta plots (Wood, 1980) and Zr-Ti/100-Y*3 (Pearce and Cann, 1973) support these observation (Fig. 9a and 9b).

The discovery of magmas that seem to be primitive (see Mgv and 3d elements) and the consistency of a large spectrum of incompatible trace elements permit us to make some model calculation about the magma source and the melting process that occurred. Consequently, a better discrimination between E-MORB and WPB can be obtained, even in the case of metamorphic rocks (Rajamani et al., 1985; Weaver et al., 1982; Bodinier et al., 1987). Ce/Sm/Yb and Ta/La/Y were modelled using the equations for non-modal equilibrium melting formulated by Shaw (1970) and the equations for non-modal fractional melting used were those of Ottonello and Ranieri (1977). Curves 1 and 4 (Fig. 10) represent trace element fractionation for non-modal equilibrium melting of a spinel

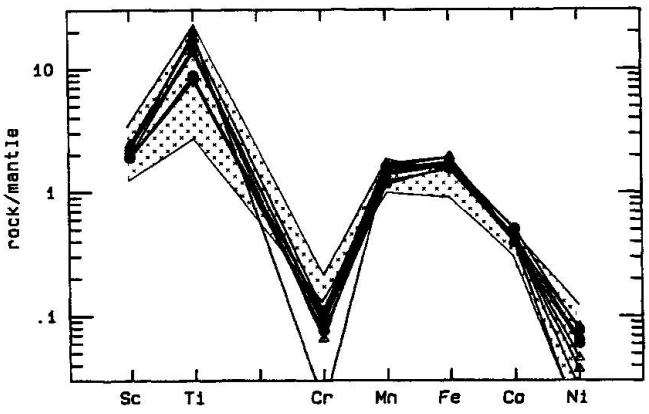

Fig. 7. 3d transition element composition of NNW and Vertana metabasalts. Normalizing values from primitive mantle of Jagoutz et al. (1979). The least-fractionated basalt field of Langmuir et al. (1977) is also reported. Symbols as in Fig. 3.

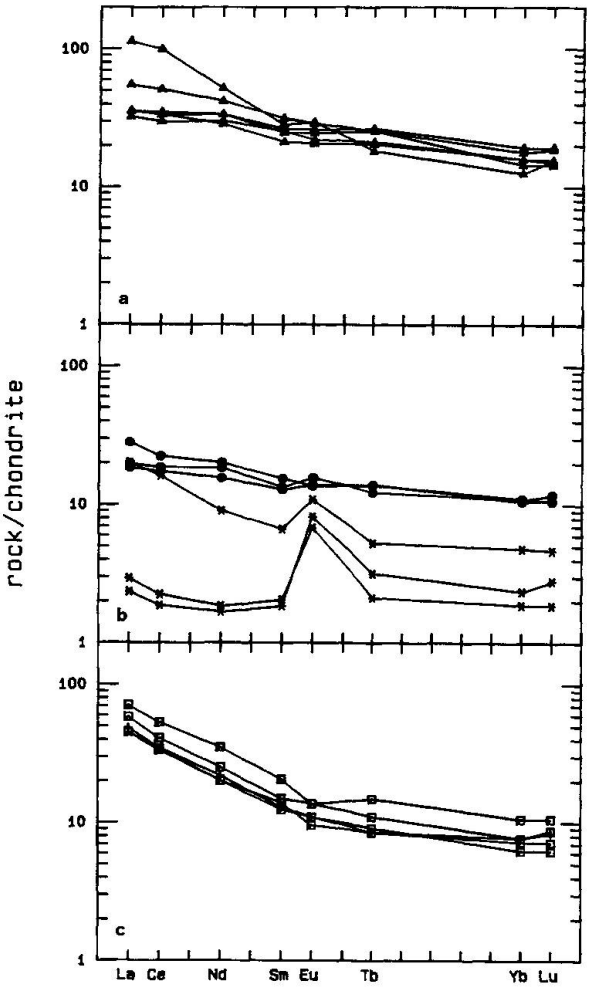

Fig. 8 Chondrite-normalized REE compositions. a) NNW basalts; b) Vertana basalts and Pennes gabbro; c) Fleres andesite. Normalizing values from BOYNTON (1984). Symbols as in Fig. 3.

peridotite (CARTER, 1970; PRESNALL et al., 1979) and of a garnet peridotite respectively (CHEN, 1971; MYSEN, 1976) source. Curves 2-3 and 5-6 represent trace element fractionation for non-modal fractional melting of spinel and garnet peridotite sources respectively (see the caption to Fig. 10 for details). Curve 7 represents the REE evolution for fractional crystallization of clinopyroxene and olivine according to the Rayleigh law.

Modal compositions of the mantle source and the melting proportions of the solid phases are taken from the compilation in OTTONELLO et. al (1984), and they are given in the caption to Fig. 10. The REE partition coefficients used for the peridotite assemblages are taken from OTTONELLO et al. (1984). The Y partition coefficients are from FREY et al. (1978). The Ta partition coefficient were evaluated from $D_{Ta}^{cpx}/D_{La}^{cpx}$ and D_{Ta}^{ol}/D_{La}^{ol} in VILLEMANT et al. (1981) and from $D_{La}^{opx}/D_{La}^{cpx}$ in FREY et al. (1978). D_{Ta}^{gar} was arbitrarily set at 0.001 in order to fit the arrangement of bulk partition coefficients for a garnet bearing mantle residue according to Wood (see Table 1 in WOOD, 1979). The $D^{cpx/melt}$ and $D^{ol/melt}$ for curve 7 are from HENDERSON (1982).

The comparison between the computed compositions and the metabasalts studied is carried out by means of binary diagrams where REE, Ta, La and Y are normalized (e.g. La_o) to the primitive mantle relative abundances of WOOD (1979) (Figs. 10a and 10b). These diagrams reproduce two of the three coordinates of the ternary dia-

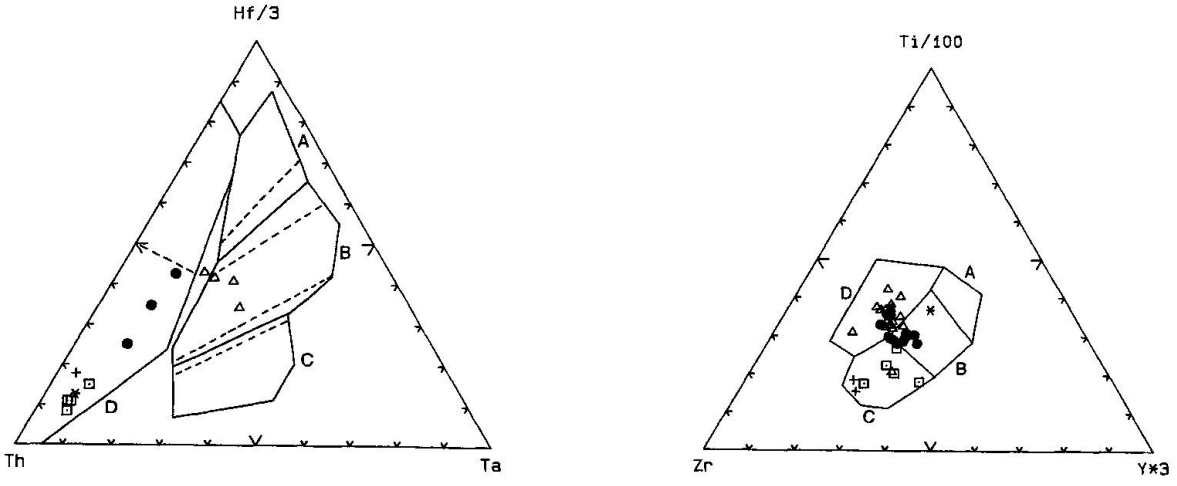

Fig. 9 Th-Hf-Ta and Ti-Zr-Y compositions of the amphibolites studied compared with the fields representing magmas which erupted in different tectonic settings. a) A - N-type MORB; B - E-type MORB and tholeiitic Within Plate Basalts (WPB); C - WPB; D - Magma series at destructive plate margins; according to WOOD (1980). Samples with Mg-value > 0.5 are shown. b) A - Island-Arc Basalts (IAB); B - Ocean Floor Basalts (OFB), Calcalkali basalts (CAB) and IAB; C - CAB; D - WPB; according to PEARCE and CANN (1973). Symbols as in Fig. 3.

a

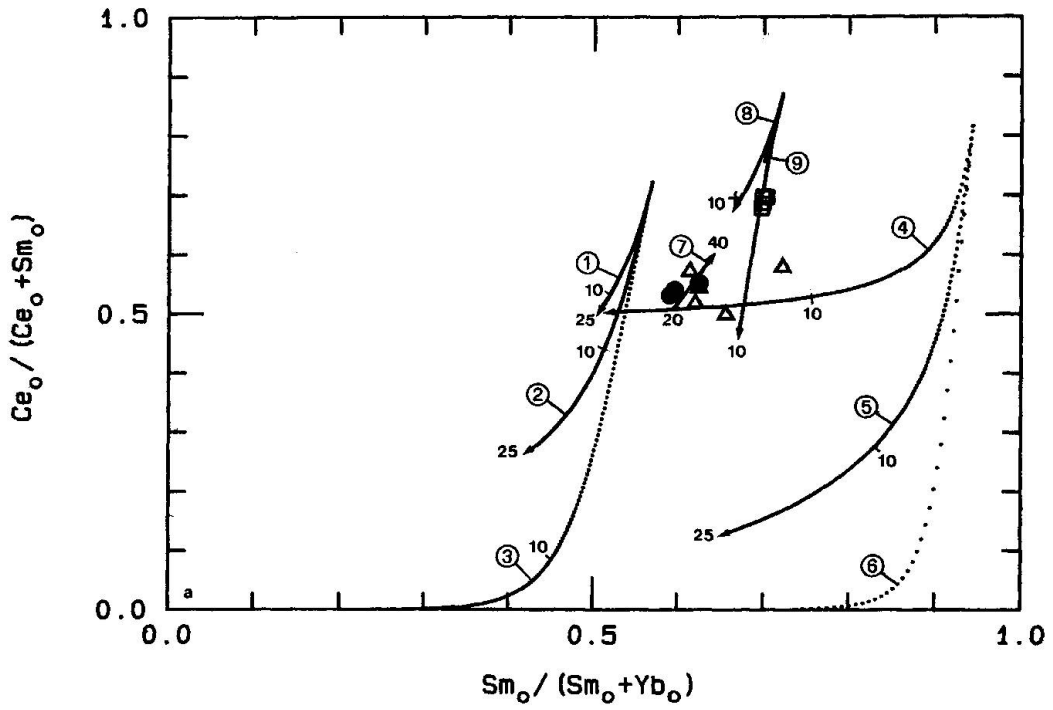

b

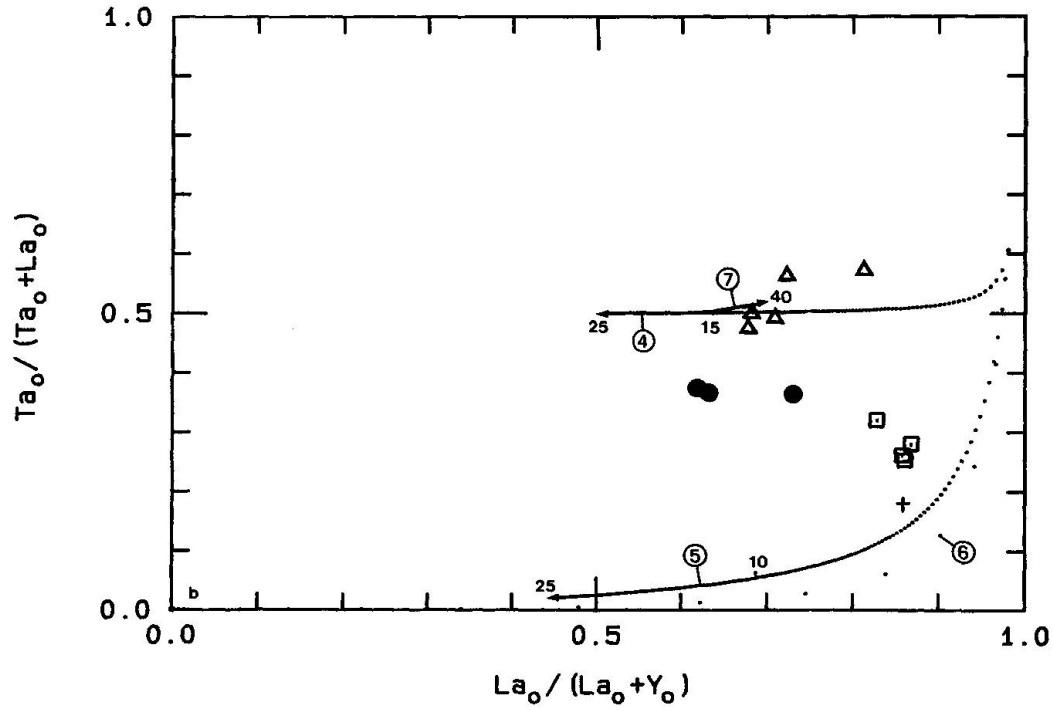

Fig. 10 a) Ce-Sm-Yb and b) Ta-La-Y relative fractionations in the rocks studied compared with computed distributions in melting liquids: curves 1, 2, 3 represent non-modal meltings of a spinel peridotite source (1: equilibrium melting; 2: fractional melting, accumulated increments of liquid; 3 - fractional melting, separated increments of liquid). Melting coefficients are: Pcpx=0.73, Popx=0.54; Pol=-0.42; Psp=0.15 (PRESNALL et al., 1979). Curves 4, 5, 6 correspond to non-modal meltings of a garnet peridotite source (4, 5, 6 as 1, 2, 3 respectively). Melting coefficients are: Pcpx=0.42; Popx=0.24; Pol=-0.09; Pgar=0.44 (MYSEN, 1976). The Ta partition coefficient evaluated (see text) are: D cpx/melt=0.01; Dopx/melt=0.0005; Dol/melt=0.0005; Dgar/melt=0.001. Curve 8 and 9 represent the distribution for non-modal melting of a hydrous garnet peridotite (MYSEN, 1982). Numerals on the curves refer to the percentage of melting.
Curve 7 corresponds to 40% fractional crystallization of 0.7% clinopyroxene + 0.3% olivine.
Normalizing values are from WOOD (1979) and BOYNTON (1984). Coordinates of the plots according to the suggestions of OTTONELLO et al. (1984). Symbols as in Fig. 3.

grams from OTTONELLO et al. (1984); thus preserving all the advantages pointed out by these authors, namely: a) eliminating the dependence of the plot of a certain composition from the source/chondrite enrichment factor and b) reducing the influence of the uncertainties of crystal/liquid partition coefficients. The source plots at the centre of the diagram, whatever its composition.

The least differentiated metabasalts closely fit the curves representing the liquids from garnet peridotite melting. A process of equilibrium partial melting probably occurred. A degree of about 20% of partial melting is suggested by the REE. Ta, La, Y computations seem to indicate a somewhat lower degree of equilibrium partial melting (≈15%), but this result is strongly influenced by the high D_y^{gar} The deviation from equilibrium melting curves can be explained by fractional crystallization of clinopyroxene and olivine; this is consistent with major and trace element such as CaO-FeO*/MgO and Cr-Ni.

Apart from the percentage of partial melting obtained, a garnet bearing source suggests a close affinity of NNW metabasalts to Within Plate Basalts.

THE VERTANA BASALTS: A POSSIBLE OROGENIC SERIES

The Vertana (meta-)basalts occur as intercalations, ca. 100 metre thick, within a staurolite phyllite-micaschist basement. They are characterized by low TiO_2 and P_2O_5 (Fig. 4) and relatively high Al_2O_3 (≈16-17%). In the R1-R2 grid (Fig. 3), a more basic character is apparent with respect to the NNW-amphibolites. High R2 numbers correlate with relatively high Mg and Al contents. These features suggest a possible analogy with "high-Al basalts" and/or with island-arc tholeiites (PERFIT et al., 1980). The TiO_2/P_2O_5/MnO ratios (MULLEN, 1983) are compatible with this hypothesis.

3d elements contents and Mgv again indicate that these basalts have relatively primitive compositions (Fig. 7). The Vertana metabasites have high Cr and Ni contents (320 and 160 ppm) compared to most other island-arc rocks, but similar values are known for some high Mg-value rocks from the New Britain Island Arc Basalt Reference Suite (BASALTIC VOLCANISM STUDY PROJECT, 1981). They also have a low absolute content of incompatible elements (Fig. 4b). The Ta, P and Ti negative anomalies, along with Ta/Hf and Th/Ta ratios (TREUIL and JORON, 1975), imply some calcalkaline affinity of these products. The Zr/Ti/Y ratios tend to confirm this conclusion (Fig. 9).

The REE trend (Fig. 8b) does not differ substantially from that of the NNW-amphibolites and modelling again suggests derivation by equilibrium partial melting of a garnet peridotite source (Fig. 10a). However, other elements whose behaviour is peculiar, e.g. Ta, cannot be modelled easily using such a single stage model. In fact, in order to obtain $Ta_o/(Ta_o+La_o)$ values ≤ 0.5 in Fig. 10b it is necessary to assume either $D_{Ta}^{gar} \gg D_{La}^{gar}$ or a mantle source with a higher La-Ta ratio («metasomatized mantle»).

THE PENNES GABBRO

This body is remarkable in the Austroalpine terrain of the Eastern Alps in that primary magmatic textures are clearly conserved in its interior, despite the fact that it underwent deformation in both the Hercynian and Alpine orogeneses. In part it appears to have been a plagioclase orthocumulate (Fig. 2). Plagioclase cumulate is strongly confirmed by major and trace element data. Relic magmatic augite was also recorded by BRIEGLEB (1967). Thus, although these rocks underwent medium to high grade metamorphism, which led to the transformation of pyroxene into tschermakitic hornblende (unpublished electron microprobe data), some magmatic crystalline phases are preserved.

Major element contents indicate that some samples, such as those reported in Fig. 2, are characterized by high Mg values (up to 85). Within this group, some have very high Al_2O_3 (up to 20%) and very low TiO_2 (down to 0.18); others, however, have low alumina, very low alkali and MgO + FeO* up to 21 wt %. Positive Eu anomalies (Fig. 8b) confirm that a large part of the Pennes gabbro is of cumulate origin; it is thought that the high Al_2O_3 samples are dominated by cumulus plagioclase. Most samples plot in the field of tholeiitic and olivine gabbros of the R1–R2 classification and, as a whole, their composition do not differ greatly from those of the Vertana metabasalts.

Some features of the primary magma can be deduced by considering a sample with reasonable R1-R2 values (R2<2000), Mg values, Cr and Sr contents. Sample COBI 5 (olivine gabbro, Mgv=66, Cr=440 ppm) was chosen. Wood's pattern (Fig. 4b) is characterized by strong Ta, Nb, P and Ti negative anomalies. The available Ta-Nb mineral/liquid partition coefficients (VILLEMANT et al., 1981; PEARCE and NORRY, 1979) appear to exclude the generation of such negative anoma-

lies by limited fractionation of pyroxene, olivine, plagioclase (see the Eu positive anomaly in Fig. 8b) and even magnetite, due to $1<D_{Ta}^{mag}$ and $1.5<D_{La}^{mag}<3$ (SCHOCK, 1979). Thus, Ta, Nb, P and Ti negative anomalies are thought to be a primary feature of the magma. It follows that the Pennes gabbro may have been emplaced within an orogenic regime (Fig. 9).

THE FLERES ANDESITES: THE OROGENIC SERIES

This fine-grained massive amphibolite occurs as a large lensoid body up to 400 metres thick. Amphibolites from Elzenbaum (Vipiteno) are also included in this group.

The plot in the R1-R2 grid (Fig. 3), the absence of FeO* enrichment with increasing FeO*/MgO and low TiO2 (Figs. 5 and 6) are all features typical of a calcalkaline series. TiO_2 versus Mg-value and Zr, and FeO* versus FeO*/MgO (not shown) indicate that these products cannot be derived by fractional crystallization from the Vertana and/or other basic magma types previously shown. In fact the differences in TiO_2 and SiO_2 between the Fleres series and the other ones cannot be reproduced without fractionation of femics and titano-magnetite. But, it is quite unlikely to do this at constant Mg-value and Zr content (Figs. 5 and 6).

The relatively high Mg values (up to 65) (Fig. 5) for the least differentiated andesites indicate that the same Fleres andesites represent very primitive melts. In fact, according to GILL (1981), the average Mg-number (HUGHES and HUSSEY, 1976) for orogenic andesites is 60, and a Mg-number ≥ 67 can indicate primary melts.

From inspection of the Wood's diagram it would appear that also the large ion elements probably did not suffer post-magmatic variations and their behaviour is probably related to differentiation by fractional crystallization.

The LREE enrichment and the slight enrichment of intermediate as compared to heavy REE (Fig. 8c) relates the Fleres andesites to medium-K andesites (GILL, 1981). This relationship receives confirmation from a K_2O vs SiO_2 plot. The more fractionated rocks display a small negative Eu anomaly (Fig. 8c), indicative of some plagioclase fractionation. The Wood's mantle-normalized pattern (Fig. 4c) is characterized by LILE enrichment and the negative anomalies in Ta-Nb, P, Hf and Ti. The Ta/Th/Hf and Zr/Ti/Y diagrams (Fig. 9) confirm the orogenic character of the Fleres andesites.

High Cr contents and relatively high Mg values suggest, for comparative purposes, plotting these "metabasites" in $Ce_o/(Ce_o+Sm_o)$ vs $Sm_o/(Sm_o+Yb_o)$ and $Ta_o/(Ta_o+La_o)$ vs $La_o/(La_o+Y_o)$ diagrams (Fig. 10). The least fractionated magmas clearly plot away from the NNW and Vertana metabasalts, mainly because of the LREE enrichment and relative HREE depletion and also because of the Ta negative anomalies. Neverthless, the REE evolution could be modelled by using modal proportions, melting coefficients and partition coefficents for a garnet peridotite according to MYSEN (1978, 1982) (see the caption to Fig. 10). Thus the curve representing REE evolution for equilibrium melting of a hydrous garnet peridotite closely approaches the experimental data. Ta/La/Y on the contrary cannot be easily modelled by such a single stage model.

Conclusions

Most metabasites from the Upper Austroalpine nappes of the Eastern Alps underwent deformation and regional metamorphism during the Hercynian orogenesis. Since these rocks represent pre-Hercynian magmatism, they are of great intrinsic interest for the information they can provide with regard to the pre-Hercynian geodynamic environment in the Alps, which about very little has been known.

High TiO_2 (>1.8-2%), high Ta/La and Zr/Y ratios suggest that the NNW metabasites (Roja, Melag, central Venosta, Passiria valleys) were Within Plate Basalts as does the 15-20% equilibrium partial melting of a garnet bearing mantle, using REE and Ta/La/Y models.

Conversely the Vertana metabasalts have low TiO_2 ($\approx$1%) and low Ta/La, P/Zr ratios, suggesting a possible calcalkaline affinity. This also may be the case for the least fractionated products of Pennes gabbro.

Low TiO_2, distinct Ta, Nb, P and Hf negative anomalies, LREE enrichment and HREE depletion strongly support a destructive plate margin origin for the Fleres andesites. It is however uncertain whether these relate to a pre- or a sin-Hercynian magmatic event.

The presence of both anorogenic and orogenic magmatism in the Austroalpine domain and the lack of radiometric chronology on the metabasalts raises a number of questions about pre-Hercynian and Hercynian geodynamics. In particular it is very important to establish whether calcalkaline products followed or preceded anorogenic magmatism, i.e. whether the Vertana calcalkaline basalts and the Fleres an-

desites are related to the Hercynian orogenesis or to an older event such as the Caledonian orogenesis.

Field and petrographical data on the Austroalpine basement (GREGNANIN, 1980) show that the Venosta and Passiria anorogenic metabasalts are intercalated in the lower unit, i.e. in the paragneisses and the silver micaschists, whereas the Vertana calcalkaline basalts lie within the upper unit, i.e. in the phyllites. Consequently Vertana series may represent a relic of magmatic activity which related possibly to the forerunners of the Hercynian orogenic cycle, which was preceded by "within-plate" anorogenic magmatism.

An alternative hypothesis is a marginal or back-arc basin (KENNETT, 1982), such as the Tyrrhenian Sea in the western Mediterranean, where a large spectrum of magma series are erupted in a very short lapse of time (10^0-10^1 million year in magnitude).

Anyway, given our present knowledge, the absence of Ocean Floor Basalts does not support the development of a large ocean basin prior to the Hercynian orogenesis. This observation is strengthened by the very limited volume now occupied by metabasites in comparison to the metapelitic series.

Acknowledgements

I am indebted to B. Upton for critical reading of the manuscript. I wish to thank A. Gregnanin and E.M. Piccirillo for continuous help and advice. I am also very grateful to P-Y. Gillot and F. Guichard for kindly supporting my work at the Centre des Faibles Radioactivités, France. V. Trommsdorff, J.M. Lardeaux, P. Nativel are also thanked.

References

BAGGIO, P., FRIZ, C., GATTO, G.O., GATTO, P., GREGNANIN, A., JUSTIN-VISENTIN, E., LORENZONI, S., MEZZACASA, G., MORGANTE, S., OMENETTO, P., PICCIRILLO, E.M., SASSI, F.P., ZANETTIN, B., ZANETTIN-LORENZONI, E. and ZULIAN, T. (1971): Foglio 4 - Merano. Carta Geologica d'Italia. Servizio Geologico d'Italia.

BASALTIC VOLCANISM STUDY PROJECT (1981): Basaltic Volcanism on the Terrestrial Planets. Island Arc Basalt. Pergamon Press, New York, 193-212.

BELLIENI, G. and SASSI, F.P. (1981): New chemical data and a review on the South-Alpine "Pre-Hercynian rhyolitic plateau" in the Eastern Alps. In: Karamata S, Sassi FP (eds.), IGCP No. 5 Newsletter 3, 22-27.

BOYNTON, W.V. (1984): Cosmochemistry of the rare earth elements: meteorite studies. In: Henderson P. (ed.), Rare earth element Geochemistry. Amsterdam: Elsevier, 63-114.

BRIEGLEB, D. (1967): Petrographische Untersuchungen am Penser Weisshorn-Amphibolit (Sarntal, Sudtirol). T.M.P.M. 12, 23-60.

BODINIER, J-L., MORTEN, L., PULA, E. and DE FEDERICO, A.D. (1987): Geochemistry of metabasites from the Nevado-Filabride complex, Betic Cordilleras, Spain: relics of a dismembered ophiolitic sequence. Lithos. 20, 235-245.

CARTER, J.L. (1970): Mineralogy and chemistry of the Earth's upper mantle based on the partial fusion-partial crystallization model. Bull. Geol. Soc. Am. 81, 2021-34.

CHEN, J.C. (1971): Petrology and chemistry of garnet lherzolite nodules in kimberlite from South Africa. Am. Miner. 56, 2098-2110.

CONDIE, K.C., VILJOEN, M.J. and KABLE, E.J.D. (1977): Effects of alteration element distribution in Archean tholeiites from the Barberton greenstone belt. South Africa. Contrib. Mineral. Petrol. 64, 65-89.

DAL PIAZ, G.B. (1936): La struttura geologica delle Austridi. Nota III. Il sistema austroalpino nelle Alpi Breonie e Venoste e nel massiccio dell'Ortles. Nuovo schema tettonico delle Austridi della Venezia Tridentina e del Tirolo orientale. Atti R. Acc. Sc. Torino 71,1-29.

DE LA ROCHE, H., LETERRIER, J., GRANDCLAUDE, P. and MARCHAL, M. (1980): A classification of volcanic and plutonic rocks using R1R2-diagram and major element analyses - Its relationships with current nomenclature. Chem. Geol. 29, 183-210.

FRANK, W., HOINKES, G., PURTSCHELLER, F. and THÖNI, M. (1987a): The Austroalpine unit west of the Hohe Tauern: The Oetztal-Stubai complex as an example for the Eoalpine metamorphic evolution. In: Flugel HW, Faupl P (ed.) Geodynamics of the Eastern Alps. Vienna: Franz Deuticke, 179-225.

FRANK, W., KRALIK, M., SCHARBERT, S. and THÖNI, M. (1987b): Geochronological data from the Eastern Alps. In: Flugel HW, Faupl P (ed.) Geodynamics of the Eastern Alps. Vienna: Franz Deuticke, 272-281.

FREY, F.A., GREEN, D.H. and ROY, S.D. (1978): Integrated models of basalts petrogenesis: a study of quartz tholeiites to olivine melilites from South Eastern Australia utilizing geochemical and experimental petrological data. J. Petrology 19, 463-513.

GILL, J. (1981): Orogenic andesites and plate tectonics. Berlin: Springer-Verlag.

GREGNANIN, A. and PICCIRILLO, E.M. (1972): Litostratigrafia, tettonica e petrologia negli scisti austridici di alta e bassa pressione dell'area Passiria-Venosta (Alto Adige). Mem. Ist. Geol. Miner. Univ. Padova 28, 1-55.

GREGNANIN, A. and PICCIRILLO, E.M. (1974): Hercynian metamorphism in the Austridic crystalline basement of the Passiria and Venosta Alps (Alto Adige). Mem. Soc. Geol. Ital. 13, 13-27.

GREGNANIN, A. (1980): Metamorphism and magmatism in the Western Italian Tyrol. Rend. S.I.M.P. 36, 49-64.

HENDERSON, P. (1982): Inorganic Geochemistry. Oxford: Pergamon.

HOINKES, G., PURTSCHELLER, F. and SCHANTL, J. (1972): Zur Petrographie und Genese des Winnebach Granites (Oetztaler Alpen, Tirol). T.M.P.M. 18, 292-311.

HUGHES, C.J. and HUSSEY, E.M. (1976): M and Mg value. Geochim. Cosmochim. Acta 40, 485-486.

JAGOUTZ, E., PALME, H., BADDENHAUSEN, H., BLUM, K., CENDALES, M., DREIBUS, G., SPETTEL, B., LORENZ V. and WANKE, H. (1979): The abundances of major, minor and trace elements in the earth's mantle as derived from primitive ultramafic nodules. Proc. Lunar. Planet. Sci. Conf. 10th, 2031-50.

KENNETT, J.P. (1982): Marine Geology. Prentice Hall, London, 752.p.

LAIRD, J. and ALBEE, A.L. (1981): Pressure, temperature and time indicators in mafic schists: their application to reconstructing the polimetamorphic history of Vermont. Am. Jour. Sci. 281, 127-175.

LANGMUIR, C.H., BENDER, J.F., BENCE, A.E., HANSON, G.N. and TAYLOR, S.R. (1977): Petrogenesis of basalts from the Famous area: Mid-Atlantic Ridge. Earth Planet. Sci. Lett. 36, 133-156.

LEAKE, B.E. (1964): The chemical distinction between ortho- and para-amphibolites. J. Petrology 5, 238-254.

MIYASHIRO, A. (1974): Volcanic rock series in island arcs and active continental margins. Am. Jour. Sci. 274, 321-355.

MOGESSIE, A., PURTSCHELLER, F. and TESSARDI, R. (1985): Geochemistry of amphibolites from the Oetztal-Stubai Complex (Northern Tyrol, Austria). Chem. Geol. 51, 103-113.

MULLEN, E.D. (1983): $MnO/TiO_2/P_2O_5$: a minor element discriminant for basaltic rocks of oceanic environments and its implications for petrogenesis. Earth Planet. Sci. Lett. 62, 53-62.

MYSEN, B.O. (1976): Rare earth partitioning between crystals and liquid in the upper mantle. Yb. Carnegie Inst. Wash. 75. 656-659.

MYSEN, B.O. (1978): Experimental determination of rare earth element partitioning between hydrous silicate melt, amphibole and garnet peridotite minerals at upper mantle pressures and temperatures. Geochim. Cosmochim. Acta 42, 1253-1263.

MYSEN, B.O. (1982): The role of mantle anatexis. In: Thorpe RS (ed) Andesites. New York: John Wiley, 489-522.

NYSTROM, J.O. (1984): Rare earth element mobility in vesicular lava during low-grade metamorphism. Contrib. Mineral. Petrol. 88, 328-331.

OTTONELLO, G. and RANIERI, G. (1977): Effetti del controllo petrogenetico sulla distribuzione del Ba nel processo di anatessi crostale. Rend. S.I.M.P. 33, 741-753.

OTTONELLO, G., ERNST, W.G. and JORON, J.L. (1984): Rare Earth and 3d Transition element geochemistry of peridotitic rocks: I. Peridotites from the Western Alps. J. Petrology 25, 343-372.

PATERNE, M., GUICHARD, F., LABEYRIE, J., GILLOT, P-Y. and DUPPLESSY, J.C. (1986): Tyrrhenian Sea tephrochronology of the oxygen isotope record for the past 60'000 years. Mar. Geol. 72, 259-286.

PEARCE, J.A. (1975): Basalt geochemistry used to investigate past-tectonic environments on Cyprus. Tectonophysics 25, 41-67.

PEARCE, J.A. and CANN, J.R. (1973): Tectonic setting of basic volcanic rocks determined using trace element analysis. Earth Planet. Sci. Lett. 19, 290-300.

PEARCE, J.A. and NORRY, M.J. (1979): Petrogenetic implications of Ti, Zr, Y, and Nb variations in volcanic rocks. Contrib. Mineral. Petrol. 69, 33-47.

PERFIT, M.R., GUST, D.A., BENCE, A.E., ARCULUS, R.J. and TAYLOR, S.R. (1980): Chemical characteristics of island arc basalts: implications for mantle sources. Chem. Geol. 30, 227-256.

PRESNALL, D.C., DIXON, J.R., O'DONNELL, T.H. and DIXON, S.A. (1979): Generation of mid-ocean ridge tholeiites. J. Petrology 20, 3-35.

RAJAMANI, V., SHIVKUMAR, K., HANSON, G.N. and SHIREY, S.B. (1985): Geochemistry and petrogenesis of amphibolites, Kolar Schist Belt, South India: evidence for komatitic magma derived by low percentages of melting of the mantle. J. Petrology 26, 92-123.

SANDER, B. (1912): Über tektonische Gesteinsfazies. Verh. Geol. Reichsanst. 1912, 249-257.

SASSI, F.P., CAVAZZINI, G., VISONA, D. and DEL MORO, A. (1985): Radiometric geochronology in the Eastern Alps, results and problems. Rend. S.I.M.P. 40, 187-224.

SCHOCK, H.H. (1979): Distribution of rare-earth and other trace elements in magnetites. Chem. Geol. 26, 119-133.

SHAW, D.M. (1970): Trace element fractionation during anatexis. Geochim. Cosmochim. Acta 34, 237-243.

SINIGOI, S., BELTRAME, C., COLTORI, M., PRINCIVALLE, F. and SECCO, L. (1988): Petrogenesis of the Paleozoic magmatic rocks of the Carnian Alps. Mineralogy and Petrology 38, 263-276.

TERUIL, M. and JORON, J.L. (1975): Utilisation des éléments hygromagmatophiles pour la simplification de la modelisation quantitative des processus magmatiques. Exemples de l'Afar et de la dorsale médioatlantique. S.I.M.P. 31, 125-174.

VILLEMANT, B., JAFFREZIC, H., JORON, J.L., TREUIL, M. (1981): Distribution coefficients of major and trace elements; fractional crystallization in the alkali basalt series of Chaine des Puys (Massif Central, France). Geochim. Cosmochim. Acta. 45, 1997-2016.

WEAVER, B.L., TARNEY, J., WINDLEY, B.F. and LEAKE, B. (1982): Geochemistry and petrogenesis of Archean metavolcanic amphibolites from Fiskenaesset, S.W. Greenland. Geochim. Cosmochim. Acta 46, 2203-2215.

WOOD, D.A. (1979): A variably veined suboceanic upper-mantle - Genetic significance for mid-ocean ridge basalts from geochemical evidence. Geology 7, 499-503.

WOOD, D.A. (1980): The application of a Th-Hf-Ta diagram to problems of tectonomagmatic classification and to establishing the nature of crustal contamination of basaltic lavas of the british tertiary volcanic province. Earth Plan. Sci. Lett. 50, 11-30.

Manuscript received May 11, 1989; accepted June 27, 1989.